Acta Crystallographica Section F
Structural Biology and Crystallization Communications
ISSN 1744-3091

Crystallization and structural analysis of GADPH from *Spinacia oleracea* in a new form

Ana Cámara-Artigas,[a] Masakazu Hirasawa,[b] David B. Knaff,[b] Meitian Wang[c] and James P. Allen[c]*

[a]Departamento Química-Física, Bioquímica y Química Inorgánica, Universidad de Almería, Carretera Sacramento, Almería 04120, Spain, [b]Department of Chemistry and Biochemistry, Texas Tech University, Lubbock, TX 79409-1061, USA, and [c]Department of Chemistry and Biochemistry, Arizona State University, Tempe, AZ 85287-1604, USA

Correspondence e-mail: jallen@asu.edu

Received 24 July 2006
Accepted 10 October 2006

PDB Reference: GADPH, 2hki, r2hkisf.

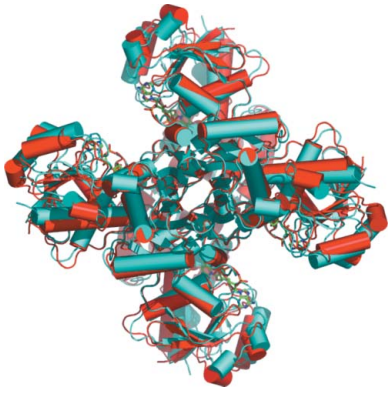

Two crystalline forms of GADPH (D-glyceraldehyde-3-phosphate dehydrogenase) from *Spinacia oleracea* were obtained using sitting-drop vapor diffusion. Despite the very low concentration of GADPH in the solutions, two crystalline forms were obtained, one of which was the previously reported *C*222 space group with unit-cell parameters $a = 155.3$, $b = 181.7$, $c = 107.6$ Å and the other of which belonged to a new space group $I4_122$, with unit-cell parameters $a = b = 120.9$, $c = 154.5$ Å. Diffraction data were measured from both native and derivatives, yielding structures at a resolution limit of 3.0 Å. Differences at the $NAD^+/NADP^+$-binding site seen in these structures compared with the previously reported structure with bound coenzyme suggest that conformational changes associated with pyridine-nucleotide binding may play a role in the regulation of this enzyme.

1. Introduction

Protein crystallization takes place through recognition processes among protein molecules. In order to obtain crystals, high purity levels of the protein are generally required, as the presence of small impurities can degrade the quality of the crystal (Caylor *et al.*, 1999). Most studies concerning the effect of impurities on macromolecular crystallization have focused on lysozyme and have shown that the impurities introduce disorder in the crystal that can be correlated with an increase in mosaicity, temperature factors and twinning. In some cases, the disorder caused by the impurities can be eliminated using a simple seeding technique (Caylor *et al.*, 1999), but the crystallization of proteins is usually carried out using the most pure form of the active protein available.

Glutamate synthase (EC 1.4.7.1), which catalyzes the two-electron reductive conversion of glutamine plus 2-oxoglutarate to two glutamates using reduced ferredoxin as the electron donor, plays a key role in nitrogen assimilation in plants, algae and cyanobacteria (Suzuki & Knaff, 2005; Vanoni & Curti, 1999). Spinach (*Spinacia oleracea*) glutamate synthase, which is the most extensively characterized of the higher plant enzymes, has been shown to be a monomeric soluble protein that is located in the chloroplast stromal space. The mature form of the protein, which contains one non-covalently bound FMN and a single [3Fe–4S] cluster as prosthetic groups, contains 1517 amino acids. The calculated molecular weight of the holoprotein is 166 189 Da (Nalbantoglu *et al.*, 1994; Dincturk & Knaff, 2001). No three-dimensional structure of the spinach enzyme or of a ferredoxin-dependent glutamate synthase from any higher plant is available. However, crystal structures are available for the monomeric ferredoxin-dependent glutamate synthase from the cyanobacterium *Synechocystis* sp. PCC 6803, an enzyme that exhibits significant sequence homology to the spinach enzyme (van den Heuvel *et al.*, 2002), and for the large subunit of an NADPH-dependent enzyme from the non-photosynthetic bacterium *Azospirillum brasilense* (Binda *et al.*, 2000). Both of these crystallized proteins contain the same prosthetic groups found in the spinach enzyme, with the FMN and [3Fe–4S] cluster arranged in similar spatial orientations in the two structures. While the two crystallized proteins have been expressed as recombinant proteins in *Escherichia coli*, this has not yet been accomplished for the spinach enzyme. The

Table 1
Data-collection statistics.

Data were collected at the Stanford Synchrotron Radiation Laboratory (wavelength 1.08 Å). Values in parentheses are for the outermost 0.1 Å resolution shell.

	*C*222	$I4_122$
Unit-cell parameters		
a (Å)	155.3	120.9
b (Å)	181.7	120.9
c (Å)	107.6	154.5
Resolution (Å)	30–3.0	40–3.0
Total observations	47405 (7085)	97911 (14141)
Unique reflections	20526 (3092)	12157 (1729)
$\langle I/\sigma(I)\rangle$	6.4 (3.8)	20.1 (4.1)
Completeness (%)	72 (78)	99.9 (100)
$R_{\rm merge}$ (%)	13 (23)	7.6 (42.8)

successful purification protocol developed for the spinach-leaf protein takes advantage of the enzyme's specificity for ferredoxin as an electron donor by incorporating a ferredoxin-affinity chromatography procedure in the last step in the purification procedure.

During our attempts to crystallize spinach glutamate synthase, we obtained crystals of another protein, D-glyceraldehyde-3-phosphate dehydrogenase (GADPH). GADPH is a soluble enzyme present in spinach-leaf chloroplasts that catalyzes the formation of 1,3-biphosphoglycerate from glyceraldhyde-3-phosphate and inorganic phosphate in an $NADP^+$-dependent two-electron oxidation. While GADPH does not bind ferredoxin, the enzyme has been shown to be part of a complex that includes an enzyme, ferredoxin:$NADP^+$ reductase (FNR), that binds ferredoxin with high affinity (Suss *et al.*, 1993). This enzyme complex is thought to facilitate channeling of NAPDH/$NADP^+$ between Calvin-cycle enzymes. Two isoforms of chloroplast GAPDH exist in higher plants: a heteromeric *AB* isoform and a homotetrameric A_4 isoform. The A_4 isoform participates in the formation of a supramolecular complex that contributes to light-dependent modulation of the overall regulation of photosynthetic metabolism (Scheibe *et al.*, 2002). The crystallization and structure determination of the tetrameric A_4 isoform of spinach GAPDH, with an overall molecular weight of 145 kDa, has been reported (Fermani *et al.*, 2001; Sparla *et al.*, 2004). The crystals were grown using vapor diffusion with the reservoir containing 1.0–1.5 *M* ammonium sulfate and the protein present at a concentration of 5 mg ml^{-1} in a solution consisting of 12.5 m*M* potassium phosphate, 0.5 m*M* NADP, 0.5–0.75 *M* ammonium sulfate and 50 m*M* Tris–HCl pH 7.5–8.5. The resulting crystals belong to space group *C*222, with unit-cell parameters *a* = 140.6, *b* = 185.6, *c* = 106.4 Å, and diffract to a resolution limit of 3.0 Å. In addition to this structure of the A_4 isoform complexed with $NADP^+$, structures have also been determined of the isoform complexed with NAD^+ and of various mutants in the same crystal form (Sparla *et al.*, 2004).

Here, we report that crystallization trials of the ferredoxin-dependent glutamate synthase from spinach leaf resulted in the crystallization of two crystal forms of the A_4-GAPDH isoform. The resulting two crystal forms of the $NADP^+$-free enzyme have been used to solve the structure of the apo form of this GAPDH isoform to a resolution of 3.0 Å. In this paper, we describe these forms and report on the structures.

2. Materials and methods

2.1. Protein crystallization

Spinach glutamate synthase (A_{438}:A_{278} = 0.112) was purified from spinach leaves and stored as described previously (Hirasawa & Knaff, 1985, 1993). Protein concentrations were estimated using the absorbance at 438 nm, assuming an extinction coefficient of 19.5 mM^{-1} cm^{-1} and a molecular weight of 160 kDa. The protein purity was estimated by three independent methods, using the

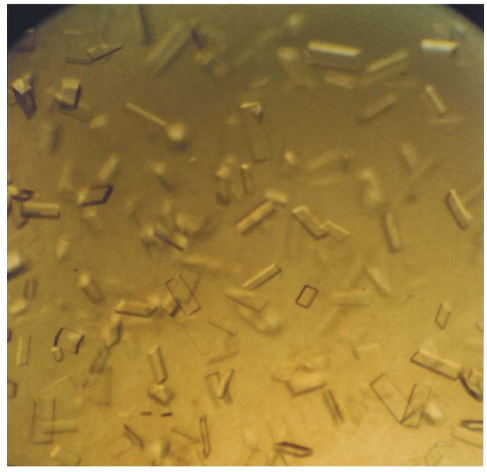

(*a*)

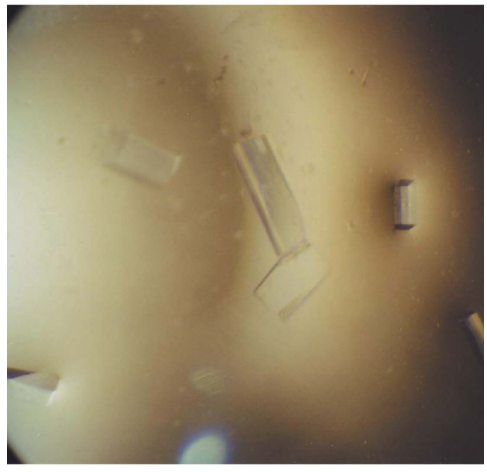

(*b*)

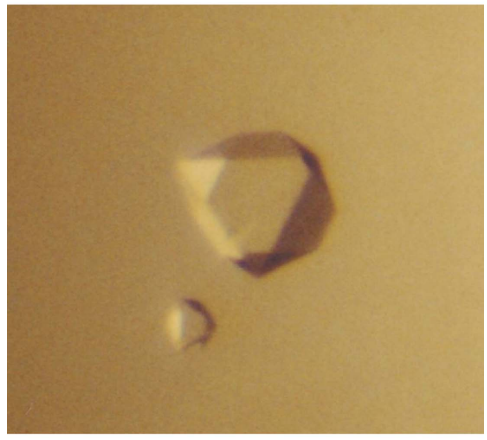

(*c*)

Figure 1
(*a*) Crystal form I grown in 2% polyethylene glycol 10 000 and 1 *M* sodium chloride pH 7 at 277 K after three weeks. (*b*) Crystals obtained by macroseeding are larger in size, with a maximal length of 1 mm, and diffract to a higher resolution limit (2.6 Å). (*c*) Crystal form II grown in 2% polyethylene glycol 10 000 and 0.6 *M* lithium sulfate pH 7 at 277 K after three weeks.

A_{280}:A_{438} absorbance ratio, the enzymatic activity and Coomassie-stained SDS–PAGE gels.

The purified protein was dialyzed into a crystallization buffer consisting of 100 m*M* tricine–KOH pH 7.5, 100 m*M* NaCl, 1 m*M* 2-oxoglutarate and 0.1% β-mercaptoethanol and was then concentrated to approximately 100 mg ml^{-1} using a Microcon YM-50 (Amicon). Crystallization was performed in 24-well plates using the sitting-drop vapor-diffusion method at room temperature. Conditions were initially screened using Crystal Screen I and II reagent kits (Hampton Research). Three different conditions yielded microcrystals: condition No. 12 [0.2 *M* magnesium chloride, 0.1 *M* Na HEPES pH 7.5, 30%(*v*/*v*) 2-propanol], condition No. 17 (0.2 *M* lithium sulfate, 0.1 *M* Tris–HCl pH 8.5, 30% polyethylene glycol 4000) and condition No. 49 [1.0 *M* lithium sulfate, 2%(*w*/*v*) polyethylene glycol 8000] from Crystal Screen I. Crystallization conditions were optimized and the best crystals were obtained using 2–5% PEG 10 000, 0.4–0.6 *M* lithium sulfate or 0.8–1 *M* sodium chloride. Typically, 40 µl droplets were prepared by mixing 20 µl protein solution and 20 µl reservoir solution and the mixture was vapour-equilibrated against 1 ml reservoir solution. Small crystals of less than 50 µm in size appeared after two weeks.

The size of all of the crystals was increased to approximately 1.0 mm using macroseeding techniques (Fig. 1). For macroseeding, an equilibrated protein solution was obtained by preparing the protein and reservoir solutions as described above for crystallization and allowing the solutions to equilibrate undisturbed for 1 d. After 1 d, the cover slip was removed and one or two small crystals that had been previously grown and soaked in serial dilutions of the reservoir solution were transferred to the equilibrated protein solution. The cover slip was then replaced and the crystals were allowed to grow without further manipulation.

2.2. Data collection and analysis

Preliminary diffraction data sets were collected at room temperature using a Rigaku RU-200HB rotating copper-anode X-ray generator operated at 50 kV and 100 mA (Cu $K\alpha$, λ = 1.5418 Å) with an R-AXIS IIC image-plate detector. Intensity data were indexed, integrated and scaled with the *HKL* programs *DENZO* and *SCALEPACK* (Otwinowski & Minor, 1997). Native data sets were measured to a resolution limit of 3.5 Å. To allow a more detailed analysis, higher resolution data were collected using synchrotron radiation with a wavelength of 1.08 Å at beamline 7-1 of the SSRL on a MAR Research image plate (320 mm). Synchrotron data were processed using the *MOSFLM* package (Leslie, 1999) and scaled with *SCALA* (Collaborative Computational Project, Number 4, 1994). For these measurements, crystals were immersed in a freezing solution for 5–10 s, picked up in a loop and then flash-cooled in liquid nitrogen before mounting in the goniometer under a stream of nitrogen gas cooled to 100 K. A mixture of 10% glycerol and reservoir solution was used as cryoprotectant.

The crystals were found to grow under two different crystallization conditions that each yielded a different space group. Form I crystals grew using lithium sulfate as a precipitant and have a pyramidal morphology. The form I crystals belong to the tetragonal space group $I4_122$, with unit-cell parameters $a = b = 120.9$, $c = 145.5$ Å. The form II crystals grew using sodium chloride as a precipitant and have a rectangular morphology. The form II crystals belong to the orthorhombic space group $C222$, with unit-cell parameters a = 155.3, b = 182.7, c = 107.6 Å. Space-group assignments for the two forms were made based upon the agreement of the intensities of symmetry-related reflections and from systematic absences. Data-collection statistics are given in Table 1.

2.3. Protein identification and structure refinement

Placement of a single glutamate synthase protein with a molecular weight of 160 kDa within the unit cell of either of the two forms was possible, as analysis of form I crystals, which have a unit-cell volume of 3 040 000 Å^3, yields a Matthews coefficient of 2.4 Å^3 Da^{-1} and a solvent content of 48%, while analysis of the form II crystals, which have a unit-cell volume of 2 330 000 Å^3, yields a Matthews coefficient of 1.82 Å^3 Da^{-1} and a solvent content of 32% (Matthews, 1968).

In order to obtain the phases by isomorphous replacement, Patterson maps were analyzed using the derivative data (data not shown). For form I, these maps show Harker lines that predict the presence of a binary axis in the unit cell and a putative space group $I4_122$. Moreover, a self-rotation map shows the clear presence of a binary axis (Fig. 2). However, the presence of two proteins in the unit cell would yield a Matthews coefficient of 1.2 Å^3 Da^{-1} that would require a very tight packing of the protein. These facts, together with the lack of success in phase determination by molecular-replacement

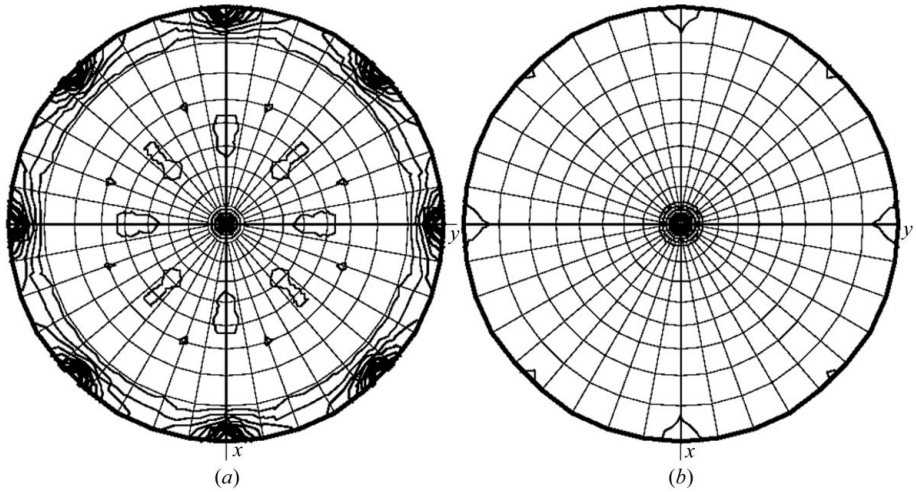

Figure 2
Self-rotation function calculated with the GADPH tetragonal crystal form employing data between 9.0 and 21 Å resolution with a 30.0 Å radius of integration. Self-rotation searches with angles of (*a*) κ = 180° and (*b*) κ = 90° were used to identify fourfold and twofold rotation angles, respectively. The presence of fourfold and twofold crystallographic symmetry is evident from the very strong peaks in the plots. The plots are contoured starting at 1σ with steps of 0.5σ.

methods using known glutamate synthase structures, led us to re-examine the identity of the protein in the crystals. MALDI–TOF analysis of the crystals together with SDS–PAGE analysis of the dissolved crystal shows the presence of a single protein with a molecular weight of 36 kDa, a value that is not consistent with the known 160 kDa molecular weight of spinach glutamate synthase. Thus, a search was conducted to find the true identity of the protein that had crystallized.

The space group of the form I crystals, $I4_1$ or $I4_122$, is atypical for protein structures, with only 148 structures belonging to space group $I4_1$ and 193 to space group $I4_122$ of the over 37 000 structures deposited in the PDB. A search of crystal structures with the same space group and unit-cell parameters resulted in two structures of the GADPH from *E. coli*, with one in space group $I4_1$ (PDB codes 1dc3 and 1dc4) and one in $I4_122$ (PDB code 1s7c). A molecular-replacement search using the 1dc3 coordinates in *MOLREP* (Vagin & Teplyakov, 1997) yielded a solution with an *R* factor of 0.46. Using the coordinates of the GADPH from spinach (PDB code 1rm4) in space group $I4_122$ resulted in an *R* factor of 0.37. For crystal form II, use of the spinach GADPH coordinates with the *MOLREP* program yielded a solution with three molecules in the asymmetric unit and an *R* factor of 0.43. After ten cycles of restrained refinement using *REFMAC*5, the *R* factor and $R_{\rm free}$ dropped to 0.23 and 0.33, respectively. The resulting structure for the form II is a tetramer generated by crystallographic symmetry that is very similar to that reported previously (Fermani *et al.*, 2001; Sparla *et al.*, 2004) and thus no further attempts to refine the structure were made. Additional refinement of crystal form I was carried out with *REFMAC*5 using TLS parameters (Winn *et al.*, 2001). The inclusion of TLS parameters in the refinement improves the *R* factor and $R_{\rm free}$, which decrease to final values of 0.20 and 0.26, respectively. Manual building of the model against the electron-density maps was conducted with the program *Coot* (Emsley & Cowtan, 2004). Because of the limited resolution of the data, water molecules have not been placed in the structure.

Figure 3
SDS–PAGE analysis of a glutamate synthase sample containing FNR and GAPDH impurities. The proteins in the three Coomassie Brilliant Blue staining bands were identified by MALDI–TOF as having molecular weights corresponding to the known weights of (i) glutamate synthase, (ii) FNR and (iii) GAPDH. In this figure, glutamate synthase is in the higher molecular-weight region and the FNR and GAPDH are close together in the lower molecular-weight region of the gel.

3. Results and discussion

3.1. Protein crystallization and quality of the crystals

Even though high-purity preparations of glutamate synthase were used for the crystallization trials, the only crystals produced were those of A_4-GAPDH. The preparation of glutamate synthase from spinach leaves involves a long and involved protocol that begins with an acetone precipitation of all the protein material present in the leaves, which is designed to separate all of the photosynthetic pigments from soluble proteins. After dissolving the precipitated protein and extensive dialysis to remove remaining traces of acetone, the resulting protein concentrate is purified by an alternating sequence of ion-exchange and size-exclusion chromatographic approaches (Hirasawa *et al.*, 1989). The final step in the purification protocol is affinity chromatography on a Sepharose column to which spinach ferredoxin has been covalently attached (Hirasawa *et al.*, 1989). In typical preparations, the specific activity of the glutamate synthase applied onto the ferredoxin-affinity column is approximately 10 units mg^{-1} and the pooled fractions exhibiting glutamate synthase activity typically have a specific activity of approximately 50 units mg^{-1} (*i.e.* a fivefold increase in specific activity). Despite this extensive purification procedure, FNR activity can be detected in some glutamate synthase preparations and in some cases FNR can be detected as a Coomassie-stained band after SDS–PAGE electrophoresis (Fig. 3). This 35 kDa impurity can easily removed by size-exclusion chromatography equilibrated at high ionic strength because of the very large difference in molecular weight between glutamate synthase and FNR. This is not the case for any GADPH bound to FNR that may be present as an impurity. Although high ionic strength causes dissociation of GAPDH from the complex containing FNR, the relatively small difference in the molecular weights of glutamate synthase (160 kDa) and the tetrameric form of GAPDH (145 kDa) limits the effectiveness of the separation of GAPDH from glutamate synthase by membrane ultrafiltration or by gel-filtration chromatography. For this reason, small amounts of GADPH can appear as a contaminant in the glutamate synthase preparations.

It has been broadly accepted that the most important feature for protein crystallization is the high purity of the protein. However, it is well documented that protein crystallization can be used as an effective tool in protein purification and many protein-purification protocols include a protein-crystallization step. Examples of proteins in which a crystallization step has been used to obtain the highest level of purity includes glycogen phosphorylase (Fischer & Krebs, 1958), cytochrome c_2 (Bartsch, 1978) and lysozyme (Judge *et al.*, 1998). Furthermore, purification by crystallization is routinely performed for low-molecular-weight compounds.

Three crystallization conditions were found to produce crystals from the glutamate synthase solutions, but in all cases a very high glutamate synthase concentration of at least 100 mg ml^{-1} was needed in order to obtain crystals. The crystals appeared after two weeks and only small crystals with a size of less than 50 µm were obtained from the initial crystallization attempts. Nevertheless, the small crystals were well faceted in all the cases and larger crystals that diffracted to a maximum resolution of 2.7 Å were grown by macroseeding techniques. Analysis of these crystals shows that they contained the protein GADPH rather than glutamate synthase. Presumably, the high protein concentration of the glutamate synthase sample resulted in concentration of the impurity, GADPH, to a sufficiently high level for crystallization of the GADPH. Thus, even though GAPDH was only a marginal component of the protein solution, the crystallization conditions used favored crystallization of the GADPH 'impurity' rather than of the dominant glutamate synthase component.

3.2. Quality of the model and overall fold of GADPH

The asymmetric unit of the *C*222 structure contains three independent proteins, which are each part of tetramer complexes generated by symmetry operations, resulting in a much larger number of atomic positions than for the $I4_122$ crystals. Initial refinement of these proteins produced an *R* factor of 22.6% and an R_{free} of 31.6%, with 2% of the residues being located in disallowed regions of the Ramachandran plot. The *C*222 structure is very similar to the previously described structure (Sparla *et al.*, 2004), with the molecules forming the functionally active tetramer being related by crystallographic symmetry. Owing to the similarity of the structure of this form to that previously reported in the literature, further refinement of this form was not pursued.

The final model of apo A_4-GAPDH in space group $I4_122$ contains one polypeptide chain with 335 amino-acid residues and four sulfate ions. The final *R* factor was 18.12% and R_{free} was 26.13%, with an average *B* factor of 38 Å^2. All residues in the model are in the allowed regions of the Ramachandran plot, with 86% being in the most favorable region. The predominant secondary structures found in the overall fold are parallel β-sheets forming a Rossmann-fold domain with a core consisting of three layers, $\alpha\beta\alpha$, and a parallel β-sheet of six strands. No electron density was found for the cofactor NAD$^+$/NADP$^+$, so this structure represents that of the apoenzyme (Fig. 4). Several sulfate ions are presumably taken up from the precipitant solution and have been modeled in the electron density. One is near Thr211, Ser152 and Thr154 at the same position as the sulfate ion found in the 1rm3 structure, which has been proposed to correspond to the position occupied by the inorganic phosphate during the phosphorylation step of the catalytic cycle (Moras *et al.*, 1975). The second sulfate ion makes contact with residues Thr183, Asp185, Arg198 and Arg234 and is located near the position of a sulfate ion previously described for the protein with bound cofactor (Sparla *et al.*, 2004). Residual electron density has also been found for two more sulfate ions located at positions corresponding to those occupied by the phosphate moieties of the cofactor NADP$^+$ in the structure of the enzyme–cofactor complex.

Alignment of the asymmetric unit of the apo A_4-GAPDH with the *A* subunit of the A_4-GAPDH–NADP$^+$ complex (Fig. 5*a*) shows significant differences, with a backbone displacement of ∼1.2 Å in the loop formed by amino-acid residues Ile33–Val39. This loop contains residues Asp35 and Thr36, which are hydrogen bonded to the O atom of the 2′-phosphate group of NADP$^+$ in the structure of the enzyme–NADP$^+$ complex. Differences in the positions of the backbone, with an average displacement of 1.0 Å, are also evident in the loop formed by residues 75–84. This loop contains Arg80, which forms part of the binding site for the NADP$^+$ cofactor. The largest, most extended differences are found in the S-loop (residues 180–203), where a backbone displacement of ∼1.8 Å is seen between the structures of the apo enzyme and its complex with NADP$^+$.

The functional form of A_4-GAPDH is a tetramer that is generated by symmetry in the $I4_122$ structure. Two major interfaces are found in the tetramer that combine to produce a buried accessible surface area of 45 583 Å^2 (*PISA* server; Krissinel & Henrick, 2005). The first interface is formed by 56 residues and involves 24 hydrogen bonds and 18 salt bridges between amino acids in the interface. The second interface involving 33 residues is formed by the S-loop and has 16 hydrogen bonds. Additionally, a disulfide bridge is formed between Cys203 and the same residue in a symmetry-related molecule in this interface, making a tetramer that can be considered to be a dimer of dimers, since monomers are bound in pairs by a disulfide bridge (Fermani *et al.*, 2001). This cysteine is not present in the *A* subunits of several GAPDHs from other plant species. For example, Cys203 is

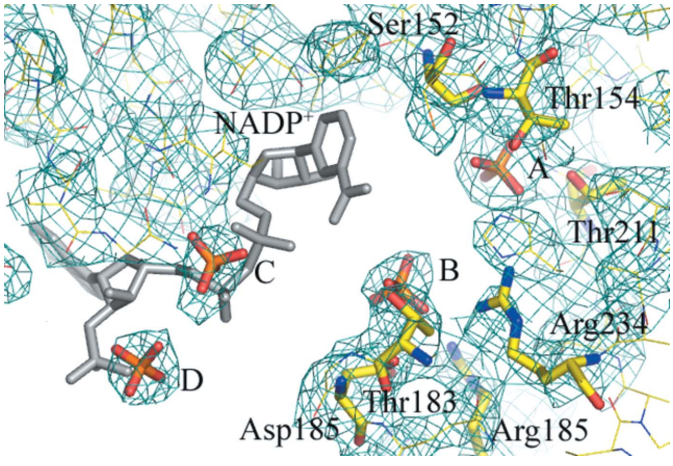

Figure 4
NADP$^+$-binding site in the apo A_4-GAPDH isoform structure showing the lack of electron density. The NADP$^+$ molecule, as it appears in the 1rm4 structure, is shown in grey. Four sulfate ions have been modelled. *A* is near Thr211, Ser152 and Thr154 and *B* near residues Thr183, Asp185, Arg198 and Arg234. *C* and *D* occupy the position of the phosphate moiety of the NADP$^+$ molecule, which is not present in this structure.

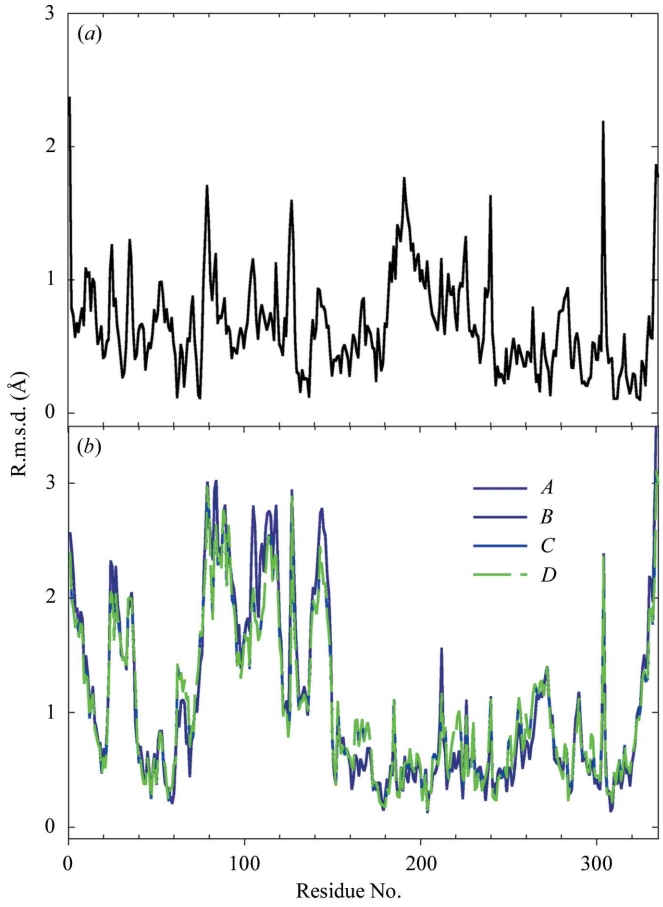

Figure 5
(*a*) R.m.s. deviation (r.m.s.d.) plot of the main-chain atoms of the apo A_4-GAPDH isoform structure (this work) and chain *A* of the A_4-GAPDH–NADP$^+$ complex (PDB code 1rm4). (*b*) R.m.s.d. plot of the main-chain atoms of the tetramer of the apo A_4-GAPDH isoform structure and the tetramer of the A_4-GAPDH–NADP$^+$ complex (PDB code 1rm4). R.m.s.d. values were calculated with the program *LSQKAB* (*CCP*4 suite; Collaborative Computational Project, Number 4, 1994).

replaced by alanine in the *B* subunit of the regulatory isoform of spinach GAPDH and in other cytosolic GAPDHs from eubacteria and eukaryotes. The presence of this extra bond in spinach A_4-GAPDH confers high stability on this chloroplast enzyme (Fermani *et al.*, 2001).

Least-squares superposition of the functional form of the enzyme on the tetrameric form of the enzyme–NADP$^+$ complex (*i.e.* the *C*222 structure; Fig. 5) shows major differences in main-chain displacement, with the largest differences of over 2.5 Å found between residues 80 and 140 and the smallest differences found in the S-loop. As can be seen in Fig. 5(*b*), significant differences exist in the orientation of the four subunits in the two structures. As a consequence of the tetramer formation, the S-loop is buried in the tetramer interface and residues 80–140 are located at the surface of the tetramer. The large differences evident for residues 80–140 arise from an expanded conformation (Fig. 6) of the tetramer of the apoprotein similar to that previously described for the Ser188 to Ala mutant, a variant that shows much a lower activity than the wild-type protein (PDB code 1rm5; Sparla *et al.*, 2004). The loops surrounding the cofactor site are found to increase the flexibility, as indicated by the previously reported lack of density in some side chains (Fermani *et al.*, 2001; Sparla *et al.*, 2004). This flexibility has been attributed to conformational changes introduced in the enzyme by cofactor binding (Moras *et al.*, 1975). The observation of the large differences in this region in the apo form of the protein compared with the NADP$^+$-bound form are consistent with a binding-induced change in the protein.

4. Conclusions

Obtaining protein samples with very high purity is broadly accepted dogma as being an essential aspect of successful protein crystallization. However, small molecules, such as sugars for example, can crystallize from low-purity solutions if favourable conditions are selected from examination of their phase diagrams. Moreover, several cases of unsuccessful crystallization of protein complexes that results in a crystallization of a single protein have been reported. Here, we report an unexpected crystallization of a minor protein present as impurity in glutamate synthase preparations. The crystals obtained belonged to two different space groups and diffracted to a sufficient quality to enable solution of the structures for both crystal forms and yielded the first structure of apo GADPH from *S. oleracea*. Differences at the NAD$^+$/NADP$^+$-binding site seen in this structure compared with the bound coenzyme previously reported suggest that these conformational changes play an important role in the regulation of this enzyme, as has been noted for the expanded tetrameric form obtained that resembles the structure of the almost inactive GADPH Ser188Ala mutant. The purification of the GADPH with glutamate synthase may be coincidental or it may arise owing to an unexpected association of these two proteins in the cell. Efforts to distinguish between these two possibilities are under way.

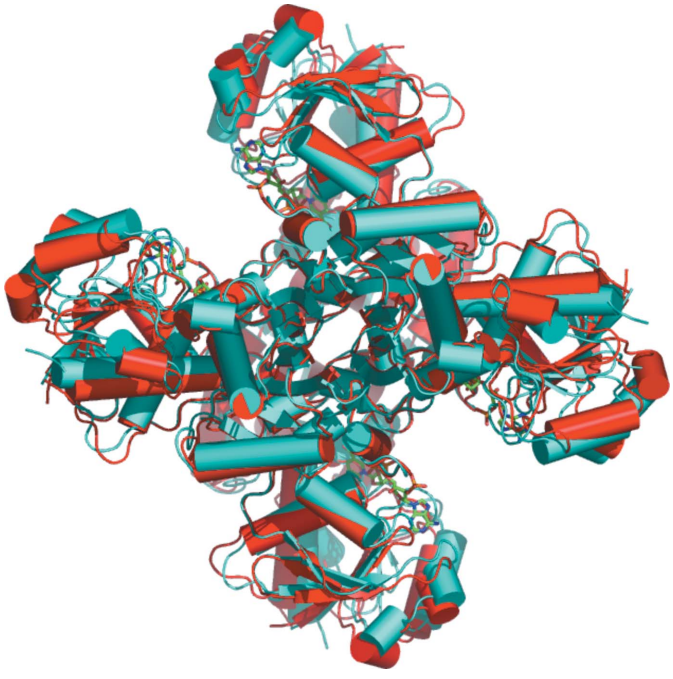

Figure 6
Superposition of the tetramers of the apo A_4-GADPH isoform (red, this work) and the A_4-GADPH–NADP$^+$ complex (cyan, PDB code 1rm4).

This work was supported by grants from the US Department of Agriculture (2003-02149 to JPA), the US Department of Energy (DE-FG02-99ER20346 to DBK) and from the Dirección General Científica y Técnica, Ministerio de Ciencia y Tecnología, Spain (BIO-2003 04274 to ACA). We thank Lisa Lauman and Dan Brune for assistance with some of the measurements.

References

Bartsch, R. G. (1978). *The Photosynthetic Bacteria*, edited by R. K. Clayton & W. R. Sistrom, pp. 249–279. New York: Plenum.
Binda, C., Bossi, R. T., Wakatsuki, S., Arzt, S., Coda, A., Curti, B., Vanoni, M. A. & Mattevi, A. (2000). *Structure*, **8**, 1299–1308.
Caylor, C. L., Dobrianov, I., Lemay, S. G., Kimmer, C., Kriminski, S., Finkelstein, K. D., Zipfel, W., Webb, W. W., Thomas, B. R., Chernov, A. A. & Thorne, R. E. (1999). *Proteins*, **36**, 270–281.
Collaborative Computational Project, Number 4 (1994). *Acta Cryst.* D**50**, 760–763.
Dincturk, H. B. & Knaff, D. B. (2001). *Mol. Biol. Rep.* **27**, 141–148.
Emsley, P. & Cowtan, K. (2004). *Acta Cryst.* D**60**, 2126–2132.
Fermani, S., Ripamonti, A., Sabatino, P., Zanotti, G., Scagliarini, S., Sparla, F., Trost, P. & Pupillo, P. (2001). *J. Mol. Biol.* **314**, 527–542.
Fischer, E. H. & Krebs, E. G. (1958). *J. Biol. Chem.* **231**, 65–72.
van den Heuvel, R. H., Ferrari, D., Bossi, R. T., Ravasio, S., Curti, B., Vanoni, M. A., Florencio, F. J. & Mattevi, A. (2002). *J. Biol. Chem.* **277**, 24579–24583.
Hirasawa, M., Chang, K. T., Morrow, K. J. Jr & Knaff, D. B. (1989). *Biochim. Biophys. Acta*, **977**, 150–156.
Hirasawa, M. & Knaff, D. B. (1985). *Biochim. Biophys. Acta*, **830**, 173–180.
Hirasawa, M. & Knaff, D. B. (1993). *Biochim. Biophys. Acta*, **1144**, 85–91.
Judge, R. A., Forsythe, E. L. & Pusey, M. L. (1998). *Biotechnol. Bioeng.* **59**, 776–785.
Krissinel, E. & Henrick, K. (2005). *Computational Life Sciences*, edited by M. R. Berthold, R. Glen, K. Diederichs, O. Kohlbacher & I. Fischer, pp. 163–174. Berlin: Springer-Verlag.
Leslie, A. G. W. (1999). *Acta Cryst.* D**55**, 1696–1702.
Matthews, B. W. (1968). *J. Mol. Biol.* **33**, 491–497.
Moras, D., Olsen, K. W., Sabesan, M. N., Buehner, M., Ford, G. C. & Rossmann, M. G. (1975). *J. Biol. Chem.* **250**, 9137–9162.
Nalbantoglu, B., Hirasawa, M., Moomaw, C., Nguyen, H., Knaff, D. B. & Allen, R. (1994). *Biochim. Biophys. Acta*, **1183**, 557–561.
Otwinowski, Z. & Minor, W. (1997). *Methods Enzymol.* **276**, 307–326.
Scheibe, R., Wedel, N., Vetter, S., Emmerlich, V. & Sauermann, S. M. (2002). *Eur. J. Biochem.* **269**, 5617–5624.
Sparla, F., Fermani, S., Falini, G., Zaffagnini, M., Ripamonti, A., Sabatino, P., Pupillo, P. & Trost, P. (2004). *J. Mol. Biol.* **340**, 1025–1037.
Suss, K. H., Arkona, C., Manteuffel, R. & Adler, K. (1993). *Proc. Natl Acad. Sci. USA*, **90**, 5514–5518.
Suzuki, A. & Knaff, D. B. (2005). *Photosynth. Res.* **83**, 191–217.
Vagin, A. & Teplyakov, A. (1997). *J. Appl. Cryst.* **30**, 1022–1025.
Vanoni, M. A. & Curti, B. (1999). *Cell Mol. Life Sci.* **55**, 617–638.
Winn, M. D., Isupov, M. N. & Murshudov, G. N. (2001). *Acta Cryst.* D**57**, 122–133.